

RESEARCH ARTICLE

Feasibility of 3D-printed middle ear prostheses in partial ossicular chain reconstruction

Anssi-Kalle Heikkinen^{1†}, Sini Lähde^{1†}, Valtteri Rissanen¹, Mika Salmi², Antti A. Aarnisalo¹, Antti Mäkitie¹, Ville Sivonen¹, Saku T. Sinkkonen^{1*}

¹Department of Otorhinolaryngology-Head and Neck Surgery and Tauno Palva Laboratory, Head and Neck Center, Helsinki University Hospital and University of Helsinki, Helsinki, Finland

²Department of Mechanical Engineering, Aalto University, Espoo, Finland

Abstract

Despite advances in prosthesis materials, operating microscopes and surgical techniques during the last 50 years, long-lasting hearing improvement remains a challenge in ossicular chain reconstruction. Failures in the reconstruction are mainly due to inadequate length or shape of the prosthesis, or defects in the surgical procedure. 3D-printed middle ear prosthesis might offer a solution to individualize treatment and obtain better results. The aim of the study was to study the possibilities and limitations of 3D-printed middle ear prostheses. Design of the 3D-printed prosthesis was inspired by a commercial titanium partial ossicular replacement prosthesis. 3D models of different lengths (1.5–3.0 mm) were created with Solidworks 2019–2021 software. The prostheses were 3D-printed with vat photopolymerization using liquid photopolymer Clear V4. Accuracy and reproducibility of 3D printing were evaluated with micro-CT imaging. The acoustical performance of the prostheses was determined in cadaver temporal bones with laser Doppler vibrometry. In this paper, we present an outline of individualized middle ear prosthesis manufacturing. 3D printing accuracy was excellent when comparing dimensions of the 3D-printed prostheses and their 3D models. Reproducibility of 3D printing was good if the diameter of the prosthesis shaft was 0.6 mm. 3D-printed partial ossicular replacement prostheses were easy to manipulate during surgery even though they were a bit stiffer and less flexible than conventional titanium prostheses. Their acoustical performance was similar to that of a commercial titanium partial ossicular replacement prosthesis. It is possible to 3D print functional individualized middle ear prostheses made of liquid photopolymer with good accuracy and reproducibility. These prostheses are currently suitable for otosurgical training. Further research is needed to explore their usability in a clinical setting. In the future, 3D printing of individualized middle ear prostheses may provide better audiological outcomes for patients.

Keywords: 3D printing; Ossicular chain reconstruction; Partial ossicular replacement prosthesis; Total ossicular replacement prosthesis; Middle ear transfer function; Laser Doppler vibrometry

[†]These authors contributed equally to this work.

***Corresponding author:**
Saku T. Sinkkonen
(saku.sinkkonen@hus.fi)

Citation: Heikkinen A-K, Lähde S, Rissanen V, *et al.*, 2023, Feasibility of 3D-printed middle ear prostheses in partial ossicular chain reconstruction. *Int J Bioprint*, 9(4): 727.
<https://doi.org/10.18063/ijb.727>

Received: December 15, 2022
Accepted: January 17, 2023
Published Online: April 4, 2023

Copyright: © 2023 Author(s). This is an Open Access article distributed under the terms of the Creative Commons Attribution License, permitting distribution and reproduction in any medium, provided the original work is properly cited.

Publisher's Note: Whioce Publishing remains neutral with regard to jurisdictional claims in published maps and institutional affiliations.

1. Introduction

In ossiculoplasty, the ossicular chain of the middle ear (ME) is reconstructed in an attempt to improve hearing. In the reconstruction, a so-called lever arm system of the ossicular chain is replaced with a prosthesis^[1]. The most common types of ME prostheses are partial ossicular replacement prostheses (PORPs) and total ossicular replacement prostheses (TORPs). Although ossicular chain reconstruction (OCR) in many cases results in better hearing soon after the operation, failures and complications may arise in the long term. Studies showed that with TORPs, for instance, after an average of 2.5 years (range 1–7 years), a good audiological outcome (air-bone gap ≤ 20 dB) was achieved only on average in 49% (range 25%–75%) of the cases^[2–15]. Because about half of the ossiculoplasties fail in the long term, there is clear need for novel prosthetic solutions.

Nowadays, there are many different designs of prostheses with various lengths, but they are not designed individually to patients' MEs. Some commercial adjustable-length prostheses have been launched and their acoustical performance has been studied with laser Doppler vibrometry (LDV)^[16]. Failures in OCR are mainly due to inadequate length or shape of the prosthesis, or defects in the surgical procedure^[17]. Too long a prosthesis can cause compression, high tension, or additional damage to the tympanic membrane or the chain structure^[17,18]. On the other hand, too short a prosthesis may tilt and move or dislocate because of changes in ventilation or static pressure in the ME^[12,19]. The intact ossicular chain has two synovial joints, and the movement of the chain is flexible and gentle. Current ME prostheses are mainly rigid and do not fully correspond to an intact ossicular chain in terms of their biomechanics. Peak amplitudes of impulsive sounds can be inhibited by a flexible ossicular chain and, therefore, replacing that with a rigid prosthesis can negatively affect the inner ear sensory structures^[16]. Rigid prostheses do not fully take into account possible changes in ME anatomy due to disease progression. The future prostheses should focus on better long-term stability^[18] and, therefore, the material should also be as well-fitting as possible. In many cases, autologous bone from the ossicles is a good option for prosthesis, but in some cases, the ossicles are absent due to the disease process, and thus, other types of ossicular chain substitutes are needed. In a preclinical study by Milazzo *et al.*^[20], cortical bone allografts were studied as OCR material. Various synthetic materials have been used in OCR, such as metal, ceramic, or plastic^[1,21,22]. Most modern prostheses are made of titanium, which is biocompatible^[4,21,23] and has well-recognized surgical and audiological properties, but the functional outcomes

(sound transmission efficacy and stability) of titanium prostheses have not been found significantly better when compared to other materials^[13,21,22,24–27].

Three-dimensional (3D) printing has become more common in various medical applications. It reduces the time and cost of manual work^[17,28]. It is used, e.g., for training and planning surgical procedures or manufacturing medical aids, tools, or implants^[29,30]. Other additive manufacturing methods can be combined with 3D printing to create complex bioartificial constructs^[31]. 3D-printed objects can be produced with different 3D printing processes and materials to achieve optimal result according to the purpose of use^[32]. In bone tissue engineering, scaffolds used in bone cell growth and differentiation can be 3D-printed^[33]. In otorhinolaryngology, microsurgical practice using 3D models is becoming more common and hearing aid molds and orbital implants have been 3D-printed for many years^[29,30].

In the development of new types of the prostheses, their adaptation to individual anatomical variations needs to be addressed. Customizing the prostheses to the patient's ME could improve the stability of the prosthesis and improve hearing outcomes by increasing the probability of a proper fit after implantation^[19]. Novel OCR prostheses' designs, materials, fabrication processes, and acoustical performance have been studied before. Hirsch *et al.*^[17] and Kamrava *et al.*^[34] utilized CT imaging and created 3D-printed PORPs in suitable shape for the imaged ME. The studies succeeded in their objective, but no information of 3D-printed prostheses' functional properties was provided. Acoustical performance of novel non-3D-printed prostheses with different designs and materials has been studied earlier with different LDV setups^[16,18,19] but also with other applications^[20,35]. Therefore, to the best of our knowledge, no information considering acoustical performance of 3D-printed ME prostheses has not been provided before.

The small size of the ME and its ossicles present challenges to imaging, 3D modeling, and printing^[17]. It is currently unknown how reliable and reproducible 3D printing is in terms of tiny ME prostheses, and what the functional properties of such prostheses are. The aim of this study was to explore the potential of 3D modeling and printing in ossiculoplasty. In this proof-of-concept study, we describe designing and 3D printing of a plastic PORP with generally used 3D printing material as well as its refinement to a second-generation prototype, and finally test its acoustical performance in middle ear transfer function (METF) in comparison to a commercial titanium prosthesis.

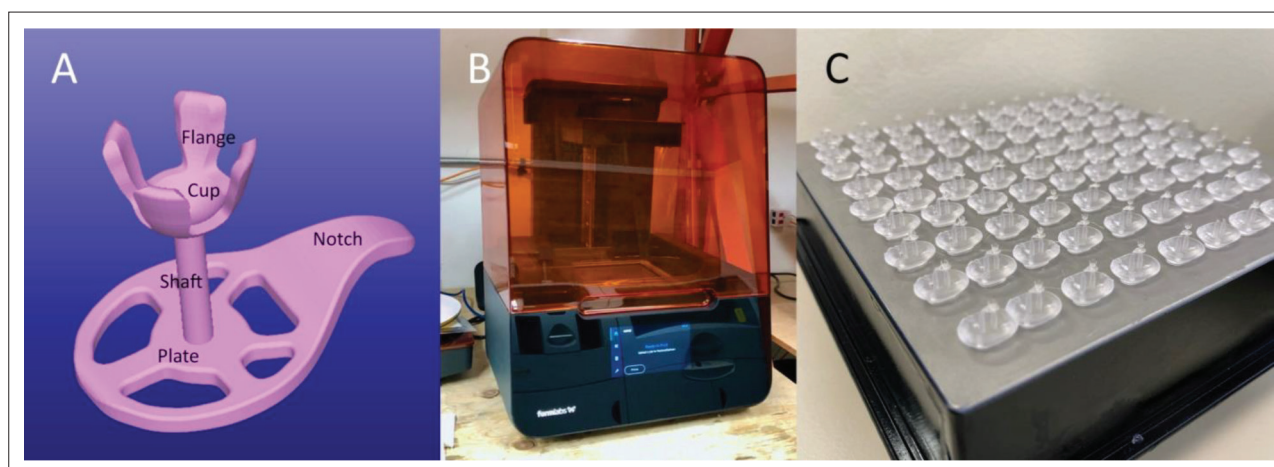


Figure 1. 3D planning and printing of PORP. (A) 3D model. (B) Form 3 3D printer. (C) Printed batches on a platform.

2. Materials and methods

2.1. Ethics and permissions

The study fulfilled the Helsinki Declaration for ethical use of human material. Institutional Review Board (IRB) at Helsinki University Hospital approved the study protocol and the use of anonymous cadaveric temporal bones in the study (approval no. §49/29.10.2020, HUS/58/2020). These temporal bones were dissected at the Department of Forensic Medicine, Helsinki University with the permission of National Supervisory Authority for Welfare and Health (permission no. 6834/06.01.03.01/2013).

2.2. Prosthesis design

The design of the 3D-printed prosthesis was inspired by a commercial titanium PORP (MNP Malleus Notch Partial Prosthesis, Heinz Kurz GmbH, Dusslingen, Germany). This specific prosthesis type is commonly used in clinical work including our surgical department. The design with malleus handle allows precise placement of the prosthesis between stapes head and malleus manubrium/tympanic membrane. PORP design instead of TORP was chosen because of the superior stability of PORP in this experimental setup. 3D models of different lengths (1.5–3.0 mm) were created with Solidworks 2019–2021 (Dassault Systèmes, France) software. The designed first-generation 3D model with a shaft diameter of 0.4 mm is shown in Figure 1A.

2.3. 3D printing

The 3D prosthesis models were saved in STL format for the print preparation software (Preform 3.9.0; Formlabs Inc., Somerville, MA). The support structures were added to the modeled prostheses using software. In addition, the dimensions of the prosthesis were marked on the support structures to identify the prostheses. The 3D printer Form 3

(Formlabs Inc., Somerville, MA; Figure 1B) was used with liquid photopolymer Clear V4 (Formlabs Inc.) as printing material. The selected layer thickness was 25 μm . The laser spot size was 85 μm and the XY resolution was 25 μm . The batches to be printed were designed and printed on a platform (Figure 1C). After printing, the parts were cleaned with FormWash (Formlabs Inc.) with pure isopropanol for 10 min and cured in FormCure (Formlabs Inc.) for 15 min at 60°C. The prostheses were numbered continuously in the order they were located on the platform. After that, the prostheses were detached from the platform and from the supporting structures manually before testing. All 3D models have been shared in a database (<https://doi.org/10.5281/zenodo.7281752>) with a full 3D printing setup file for Form 3. The experiments can be repeated with other printers with a given resolution and material.

2.4. Micro-CT imaging

To assess printing accuracy and reproducibility, 14 representative first-generation 3D-printed prostheses were imaged with micro-CT (GE, Phoenix v|tome|x s, Wunstorf, Germany; 240 kV microfocus tube, resolution 40.09 μm , 2,500 different angles). The micro-CT data were processed using Thermo Fisher PerGeos 2020.2 (Thermo Fisher, Waltham, MA). The data were segmented with watershed segmentation and converted into a surface, which was then exported to an STL file. The dimensions of the prostheses were measured with a GOM Inspect 2021 (Carl Zeiss GOM Metrology GmbH, Germany) program. Functional length and shaft diameter were measured from the images. The functional length refers to the distance from the bottom of the cup part to the outer surface of the plate.

2.5. Photo stacking

After 3D printing, selected 3D-printed prostheses were photographed by a photo stacking technique. In the

photography, the distance of the prosthesis from the camera was sequentially changed by approximately 0.1 mm by attaching the camera to a macro-focusing rail. Typically, around 30–40 photographs were taken from each prosthesis. The series of photographs, i.e., a stack of frames, was then processed by calculating the final sharp image with a high depth of field using CombineZP software (Alan Hadley, United Kingdom).

2.6. Preparation of temporal bones

Four anonymous cadaveric temporal bones were used. The temporal bones were removed from the cadaver heads as whole. No evidence of macroscopic or microscopic pathology was detected. The fresh-frozen temporal bones were thawed only once. Standard mastoidectomy was performed with a high-speed otosurgical drill (Stryker, 5400-50 Core, Kalamazoo, MI). Labyrinthectomy was then performed to gain access to the medial side of the stapes footplate (Figure 2A and B). A wide posterior tympanotomy was performed to allow inspection and manipulation of the whole ossicular chain and medial aspect of the tympanic membrane (Figure 2D and E).

2.7. Middle ear transfer function

The mechanics of the ossicular chain and the acoustical performance of the 3D-printed prostheses were determined by single-axis LDV. The measurement setup was based on Stoppe *et al.*^[18] The setup is shown in Figure 2A.

Based on pilot measurements on the transduction of sound from the tympanic membrane to the stapes footplate in an intact ME, it was determined that the METF stabilized after approximately 2 h from the beginning of the thawing process. Similarly, the lack of moisture in the ME due to evaporation started to affect the METF after 3.5 h from a thawed temporal bone. Therefore, 2 h after thawing, a speculum and an associated adapter were placed in the ear canal. An earphone (ER1, Etymotic Research Inc., Elk Grove Village, IL) and a probe microphone (ER-7C, Etymotic Research Inc., Elk Grove Village, IL) were connected to the adapter. Probe tube was inserted to the end of the speculum as close as possible to the tympanic membrane. The adapter had a sealing window that allowed visibility to the tympanic membrane. The ear canal was sealed with silicone wax. Due to sealing, the signal-to-noise ratio (SNR) was at a minimum of about 25 dB. A multisine excitation signal was used in the frequency range from 100 Hz to 5 kHz. The sound signal was generated with MATLAB (MathWorks, Natick, MA) and reproduced by the earphone through a USB sound card and an amplifier. The LDV measurements were performed at an overall level of approximately 105 dB SPL in the ear canal.

Velocity of the medial side of the stapes footplate was measured with a laser Doppler vibrometer (VibroFlex

Connect VFX-F-110, Polytec GmbH, Waldbronn, DE). Afterward the velocity was converted to displacement with Polytec Vibrometer software (Polytec GmbH). The LDV sensor head (VibroFlex Compact VFX-I-130, Polytec GmbH) was attached to the operation microscope M320 (Leica Microsystems, Heerbrugg, Switzerland) using a micromanipulator (A-HLV-MM40, Polytec GmbH), which made it easier to aim the laser beam at the measurement point marked at the medial side of the stapes footplate. The measuring range was adjusted to the smallest possible (10 mm/s) and the samples were averaged 50 times to increase the SNR of the measurements.

Cadaver temporal bones were always moistened with saline before measurements. An approximately 1 × 1 mm plastic reflective glitter was placed on the middle of the stapes footplate to improve the reflection of the laser beam (Figure 2B and C). The first measurement was performed with intact ossicular chain, followed by a measurement where incus was removed. Then, the measurement was performed with a reconstructed ME together with 3D-printed PORP or a commercial titanium PORP (Clip Partial Flexibal Prosthesis, Heinz Kurz GmbH).

The lengths of the prostheses were determined by testing different lengths for each specimen, and the most suitable prostheses (1.5, 1.75, 2, 2.25, 2.5, 2.75, and 3 mm) as deemed by the otosurgeon and the received METF results were selected for the comparisons.

2.8. Statistics

A two-way analysis of variance (ANOVA) was performed with ME transduction mode (intact ME, titanium PORP, 3D-printed PORP and incus removed) and frequency (averaged on octave bands centered around 125, 250, 500, 1,000, 2,000, and 4,000 Hz) as dependent variables and METF as an independent variable. Multiple comparisons of the means were adjusted with the Bonferroni correction. The analysis was conducted using IBM SPSS version 25 software (IBM, Armonk, NY).

3. Results

The first-generation 3D-printed PORPs (Figure 3A) were visually analyzed using an operating microscope. The printed prostheses were evaluated by their general overview, cup structure, and straightness of the shaft. With these viewpoints in mind, all prostheses were classified as successfully or unsuccessfully printed. The problems faced with the first-generation PORPs were deviations in the cup structure (Figure 3B) and broken shafts (Figure 3C). No other issues were detected. As a result, 43 of the 80 printed PORPs (54%) were classified as successfully printed.

From the successfully printed first-generation PORPs, 14 consecutive prostheses were selected by visual

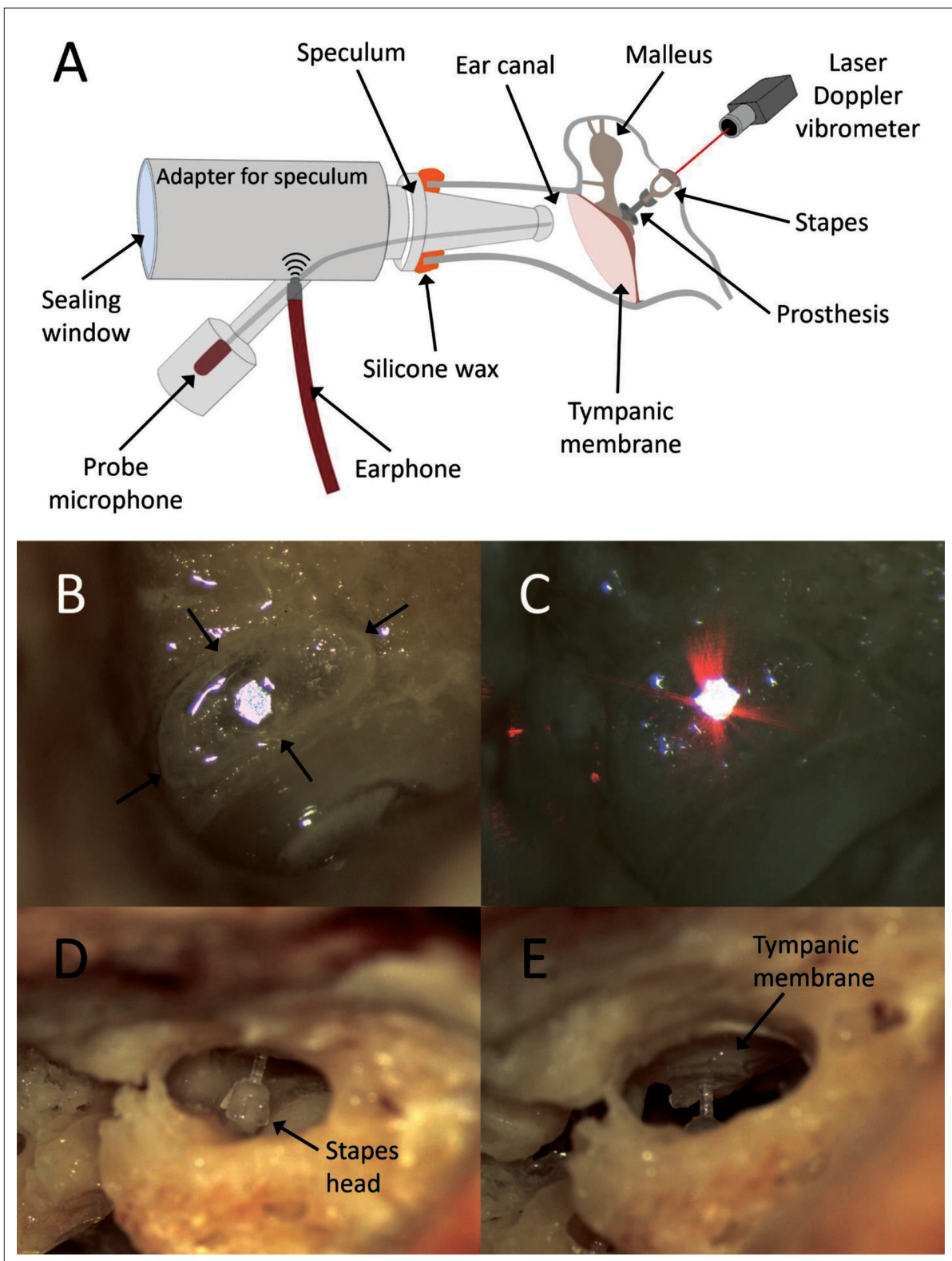


Figure 2. Functional measurement setup. (A) Functional measurement setup for measuring middle ear transfer function. (B) Stapes footplate (between arrows) seen from the medial side with mirroring glitter. (C) Laser beam directed to glitter. (D) 3D-printed prosthesis in place between stapes head and (E) tympanic membrane seen through posterior tympanotomy.

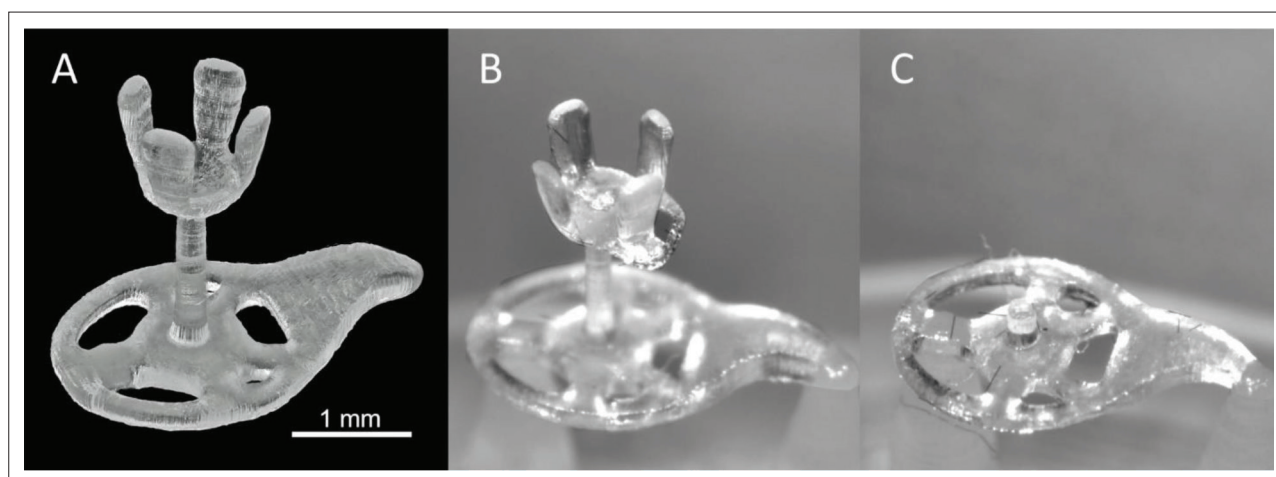


Figure 3. First-generation 3D-printed PORP. (A) Successfully 3D-printed prosthesis (macro photography by M.Sc. (Tech) Pekka Paavola). (B) Structural deviation in the cup. (C) Broken shaft.

inspection and imaged with micro-CT. After that, the dimensions of the PORPs were measured individually. In the 3D model, the shaft diameter and the functional length of the prostheses were designed to be 0.400 mm and 1.893 mm, respectively. Table 1 shows the mean measures of the 14 prostheses together with their standard deviations (SD). On average, the printed prostheses had shaft diameter 54 μm thicker and functional length 64 μm longer than in the model. The SD for shaft diameter was 21 μm and 57 μm for functional length. As for accuracy and reproducibility, the SDs of the printed PORPs as well as size differences when comparing the printed PORPs and the 3D models are close to the micro-CT's imaging resolution (40.09 μm), suggesting that 3D printing of PORPs is precise.

After visually analyzing the first-generation 3D-printed PORPs with a success rate of 54%, we decided to increase the shaft diameter from 0.400 to 0.600 mm. Also, cup flanges were made larger in order to prevent sharp edges in printing. In addition, as some of the PORPs' plates were broken when detaching them from the supporting structures, we reduced the hole sizes in the prosthesis plate. In Figure 4A, a second-generation PORP is shown in 3D model format, and, in Figure 4B, a 3D-printed second-generation PORP is photographed by the photo stacking technique. When printing this second-generation PORPs, 129 out of 130 prostheses were classified as successfully printed. Only one prosthesis was classified as unsuccessfully printed due to a broken shaft. Thus, the modifications mentioned before improved the printing success rate significantly.

The functionality of the second-generation 3D-printed PORPs was tested in LDV (Figure 4A). Figure 4D and E demonstrate a 3D-printed PORP placed between stapes head and tympanic membrane through posterior

Table 1. Accuracy of 3D printing in the first-generation PORP

3D model	Sample no.	Shaft diameter (mm)	Functional length ^a (mm)
		0.400	1.893
Prostheses	1	0.439	1.931
	2	0.432	1.935
	4	0.444	1.927
	8	0.406	2.012
	12	0.447	1.966
	13	0.480	2.075
	14	0.486	1.885
	15	0.460	1.928
	16	0.442	1.942
	17	0.474	2.062
	19	0.465	1.871
	21	0.471	1.966
	27	0.461	1.967
	30	0.444	1.929
Mean		0.454	1.957
SD		0.021	0.057
Range		0.406–0.484	1.871–2.075

14 prostheses analyzed with micro-CT with their mean and standard deviation (SD).

^aFunctional length means distance from the bottom of the cup part to the outer surface of the plate.

tympanotomy. The METF was measured with intact ossicular chain, without incus, and with a titanium Kurz Clip Partial Flexibal prosthesis or a second-generation 3D-printed PORP. In Figure 5, mean (solid line) METFs measured in different ME transduction modes are plotted with their SDs (colored area). Displacement (in nanometers;

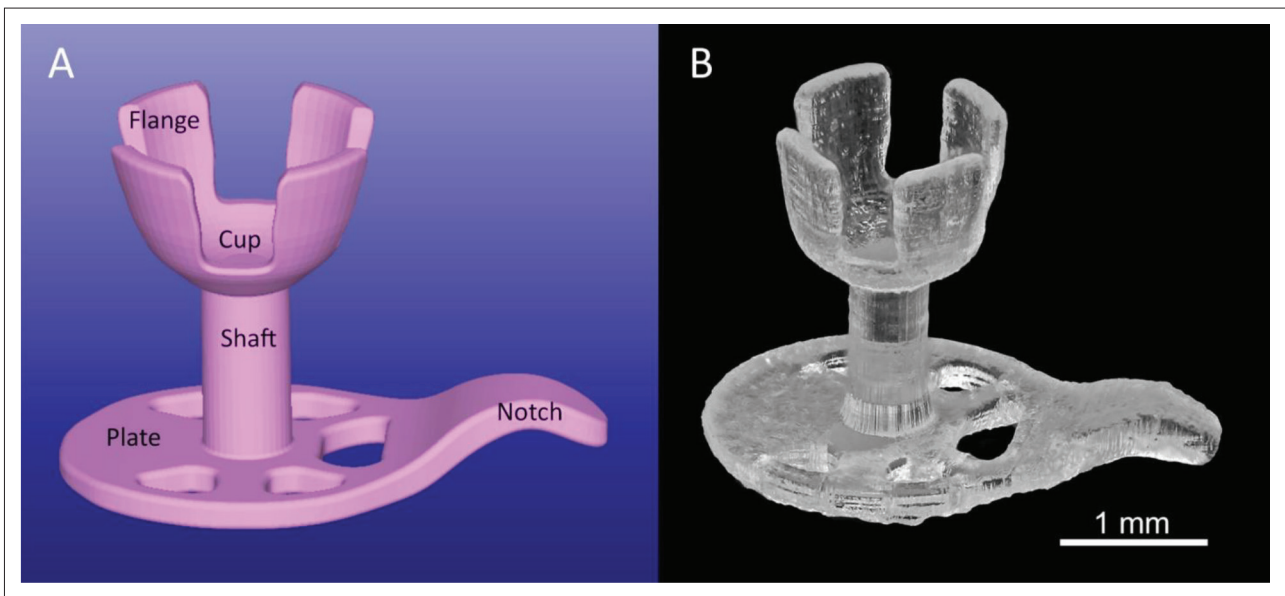


Figure 4. Second-generation 3D-printed PORP. (A) Second-generation 3D model. (B) 3D-printed prosthesis (macro photography by M.Sc. (Tech) Pekka Paavola).

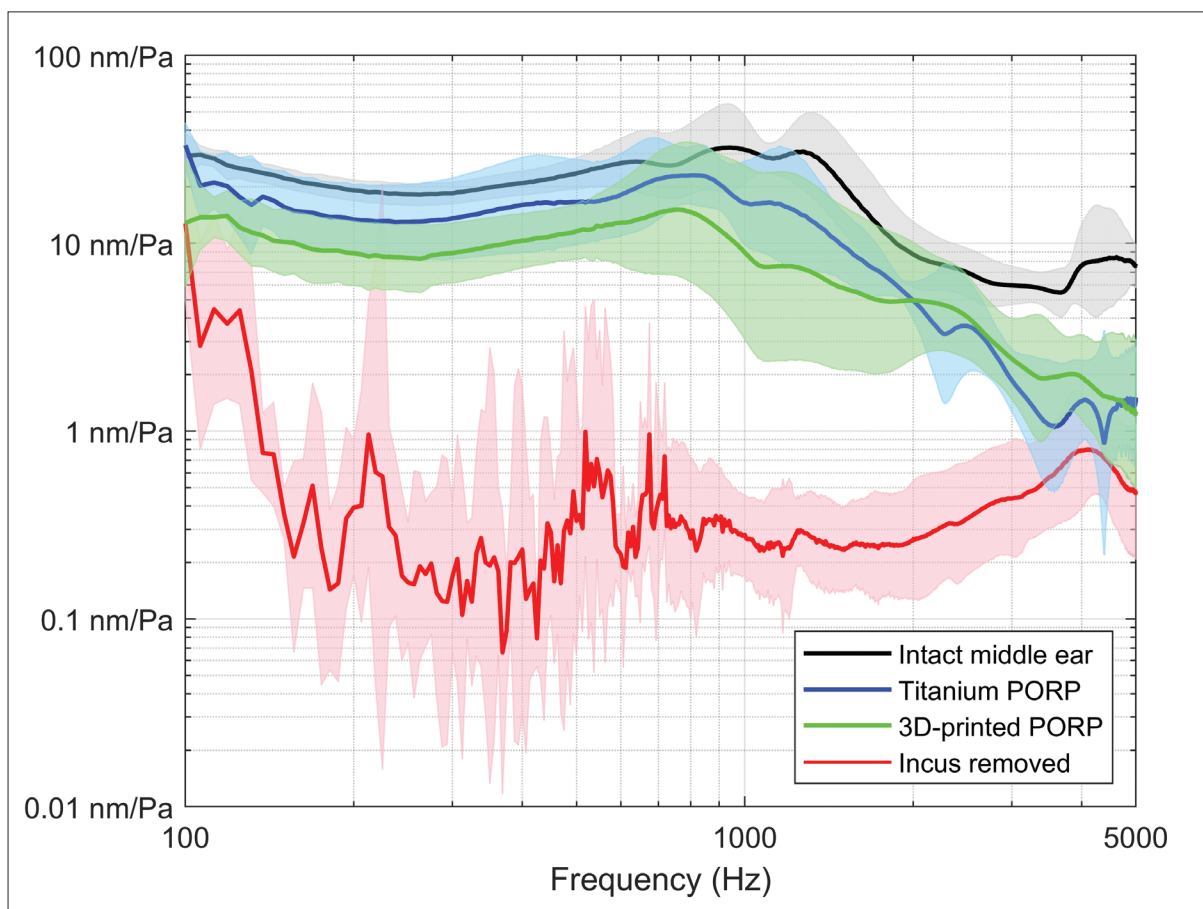


Figure 5. Middle ear transfer function (METF) in different middle ear transduction modes. Mean METF (solid line) \pm SD (colored area) across the four temporal bones are plotted for intact ossicular chain, without incus, and for titanium Kurz Clip Partial Flexibal prosthesis and for 3D-printed prosthesis.

nm) of the stapes footplate per pressure (in Pascal; Pa) in the ear canal close to the tympanic membrane is displayed on the ordinate with frequency (in Hz) on the abscissa. Each decade on the ordinate corresponds to a 20 dB change in the METF. When the incus was removed from the ME and the displacement of the stapes footplate for a given pressure was small, the METF was affected by vibration from external sources coupling to the measurement setup. This resulted in an uneven and variable response of the incus-removed measurement at low frequencies. Removing the incus decreased the METF about 40 dB at maximum. The overall shape of the METFs was similar for the intact ME and for both PORPs: displacement per pressure was relatively flat up to a resonance at around 1,000 Hz, and at higher frequencies, the METFs decreased with frequency. The two-way ANOVA revealed that there was a statistically significant interaction between the effects of ME transduction mode and frequency [$F(15,71) = 4.146, p < 0.001$]. This is seen in Figure 5, where the shape of the mean METF with the incus removed clearly deviates from the other conditions. The main effect of ME transduction mode and frequency were both statistically significant [$F(3,71) = 204.8, p < 0.001$ and $F(5,71) = 17.08, p < 0.001$, respectively]. Pairwise comparisons revealed that the METF of both the titanium and the 3D-printed PORP differed significantly from the intact ME ($p = 0.001$ and $p < 0.001$, respectively), as well as from the METF with the incus removed ($p < 0.001$ for both). However, there was no difference in METFs between the two PORP types ($p = 0.605$), suggesting that the acoustical performance of the 3D-printed PORP was equal to the commercial titanium prosthesis.

Senior otosurgeons (S.T.S. and A.A.A.) evaluated the surgical properties of the second-generation 3D-printed PORPs. The prostheses were easy to maneuver under the operating microscope. Static electric charge did not pose a problem. The prostheses, in comparison to commercial titanium prostheses, were stiffer and less flexible, and thus a bit harder to insert between the stapes head and the tympanic membrane and the malleus manubrium, even though the position and angle of the prostheses were easy to change. Thus, it was very critical to use a prosthesis with a proper length, because in the LDV setup, the tympanic membrane was intact (in contrast to a clinical situation where the tympanic membrane is lifted before prosthesis insertion). Altogether, the surgical properties of 3D-printed prostheses were acceptable, and no gross differences with the commercial titanium prostheses were noticed.

4. Discussion

Modern product development heavily utilizes 3D printing across different industries such as medical, aerospace, consumer products, military, and automotive^[36-39].

Prototyping and testing new products through 3D printing is well established. Currently, more and more applications have been seen where 3D printing is not only the prototyping method but also the actual manufacturing method. 3D printing as manufacturing fits well for spare parts, small series production, personalized products, and optimized parts^[36,38]. In addition, it offers the possibility for local manufacturing, e.g., in hospitals^[38]. In otosurgery, individualized solutions in ME prostheses may be needed to increase the likelihood of achieving better postoperative audiological outcomes in ossiculoplasty.

In this proof-of-concept study, 3D printing of second-generation PORPs with affordable desktop 3D printer and generally used 3D printing material was accurate and reproducible. All the first- and second-generation 3D-printed PORPs were made of rigid polymer. In terms of surgical maneuverability, they were considered stiffer and less flexible compared to titanium PORPs used in this study. The acoustical performance of 3D-printed PORP was similar to that of a commercial titanium PORP when comparing their METFs. In a mass-spring-damper system, the response at low frequencies is governed by stiffness, while at high frequencies, it is governed by mass. At natural frequency, the response is governed by damping. When comparing the METFs of the two PORPs in Figure 5, the response is similar in shape below 1,000 Hz. On average, the displacement for a given pressure below 1,000 Hz is approximately 1.6 times as large for the titanium PORP than for the 3D-printed photopolymer PORP. Although the difference of about 4 dB was not statistically significant in our sample, this is possibly due to the higher stiffness of titanium compared to the material used for 3D printing in this study. At high frequencies, the slope at which the METF decreases with frequency appears steeper for the titanium PORP. This may be explained by the approximately four times higher density of titanium compared to photopolymer.

When inspecting the absolute values of the METF for an intact ME measured from the inner ear side without the cochlea, the results are well in line with a study by Stoppe *et al.*^[18] (see their Figure 3B in article^[18]), being on the order of a few tens of nm/Pa. In their study, the acute pure-tone average (PTA; an average of 500, 1,000, 2,000, and 4,000 Hz) magnitude gain for a rigid TORP was 4 dB below the intact ME. Although the type of ME prosthesis was different in the present study, the corresponding PTA reduction was 8 and 9 dB for the titanium and 3D-printed PORPs, respectively. However, it should be noted that static pressure variations worsen the audiological outcomes, as illustrated in a study by Stoppe *et al.*^[18] for TORPs.

It is well known that motion of the stapes is not piston-like, and therefore, in a study by Gottlieb *et al.*^[16],

this issue combined with frequency-dependent vibration modes^[40-42] of the stapes has been solved using 3D LDV setup to measure velocity of the stapes posterior crus. In a study by Hato *et al.*^[41], an increased piston-like motion of the stapes was found at all frequencies when the cochlea was drained. In this study, velocity of the medial side of the stapes footplate was chosen to be measured using single-axis LDV setup with a mirroring glitter placed in the middle of the footplate to find movement of the stapes that was as piston-like as possible and to allow direction of the laser beam to be as repeatable as possible when changing between different ME transduction modes.

Titanium is a well-known material used in *in vivo* prostheses and compatible with bone tissue. Light and thin structures, such as the shaft of a ME prosthesis, can also be made of titanium. The costs of titanium prostheses are higher, which can affect user-friendliness^[22]. The 3D printer and polymer material used in this study could not be used to create structures as thin as those seen in the current commercial titanium prostheses. Other 3D printing processes with biocompatible materials^[32] that are already accepted for *in vivo* use could be utilized in ME prosthesis production. On the other hand, 3D printing in bone tissue engineering^[33] could be also a promising alternative solution in the future.

The 3D-printed liquid photopolymer used in this study to 3D-print prostheses is not accepted as *in vivo* prosthesis material and is thus not suitable for clinical use. However, the 3D-printed liquid photopolymer prostheses seem to be valuable practice tools for otosurgery training due to their good microsurgical usability and low production costs, as one 3D-printed PORP costs less than 5 USD. In this study, only one PORP design was used, but with 3D modeling and printing, it will be easy and cheap to fabricate different types of PORPs and TORPs for surgical training.

Based on our experience, most of the flaws of the first-generation PORPs were related to the 3D printing process itself. The laser spot size and the XY resolution of the 3D printer are the limitations to making small features. In addition, the beam is typically Gaussian distributed, and there are always reflections. One of the biggest challenges for these flaws is that in inverted vat photopolymerization, there are peel forces that affect the print as it separates from the surface of the tank. This makes printing of miniature features challenging since they typically deform or break. By widening the shaft diameter in the second-generation PORPs, we were able to find construction that could be 3D-printed more reliably.

In studies by Hirsch *et al.*^[17] and Kamrava *et al.*^[34], different types of PORPs were designed using CT imaging as an anatomical source. In the study by Hirsch *et al.*^[17],

commercial multi-slice CT (MSCT) was used, while the study by Kamrava *et al.*^[34] also used a micro-CT device. According to the study by Hirsch *et al.*^[17], the most important structures in prosthesis design were seen in dissected temporal bones with adequate resolution but in *in vivo* use, the resolution could be weaker, and thus, designing individualized ME prostheses with commercial MSCT could be hard. Micro-CT, on the other hand, cannot be utilized in clinical use because of its high radiation exposure, and therefore, imaging of ossicles with adequate effective doses for 3D printing is currently challenging due to relatively low resolution. In the future, cone-beam CT may become more common in ME imaging^[43] and it could also be considered for use in individualized prosthesis designing.

In the current study, four different temporal bones were used. Prostheses used in these bones were selected so that they fit precisely in the individual MEs. The current experimental setting enables individual anatomical ME circumstances to be taken into account. 3D printing offers the advantage to print prostheses in different sizes, and this can be availed both in surgical training and in developmental work when planning novel prosthesis design. As a consequence, 3D printing can offer a budget-friendly way in future individualized ME prosthesis production.

In the future, more studies are needed focusing on novel prosthesis designs and additive manufacturing technologies of 3D printing, especially to produce thin structures and to test their acoustical performance. Extensive material testing will also be needed if clinical applications will be pursued.

5. Conclusion

This study shows that acoustical performance and surgical maneuverability of a 3D-printed photopolymer PORP compares well with that of a commercial titanium PORP. Currently, these 3D-printed photopolymer PORPs may well be used in otosurgical training, but before possible clinical applications, several technical issues must be solved. Biocompatibility issues and utilization of printing materials already accepted for patient use must be explored. More studies are warranted concerning different additive manufacturing processes and their accuracy in printing microscopic objects, printing materials, novel prosthesis designs, and acoustical performances of the novel prostheses. In the future, with more precise imaging modalities available for patient use, individualized ossicular chain replacement prostheses could be feasible using additive manufacturing techniques with biocompatible printing materials.

Acknowledgments

We want to thank M.Sc. (Tech) Pekka Paavola for photo stacking technique photographing. We also want to thank Ph.D. Jukka Kuva (Geological Survey of Finland, Espoo, Finland) for collaboration with regard to micro-CT imaging. X-ray tomography was supported by the Academy of Finland via RAMI infrastructure project (#293109).

Funding

This study has been funded by the Tauno Palva Foundation, the Helsinki University Hospital Research Fund and the Academy of Finland Grant 325509.

Conflict of interest

The authors declare that the research was conducted in the absence of any commercial or financial relationships that could be construed as a potential conflict of interest.

Author contributions

Conceptualization: All authors

Formal analysis: Anssi-Kalle Heikkinen, Sini Lähde, Valtteri Rissanen, Antti Mäkitie, Ville Sivonen, Saku T. Sinkkonen

Investigation: Anssi-Kalle Heikkinen, Sini Lähde, Valtteri Rissanen, Mika Salmi, Ville Sivonen, Saku T. Sinkkonen

Supervision: Ville Sivonen, Saku T. Sinkkonen

Writing – original draft: Anssi-Kalle Heikkinen, Sini Lähde, Ville Sivonen, Saku T. Sinkkonen

Writing – review & editing: All authors

Ethics approval and consent to participate

The study fulfilled the Helsinki Declaration for ethical use of human material. Institutional Review Board (IRB) at Helsinki University Hospital approved the study protocol and the use of anonymous cadaveric temporal bones in the study (approval no. §49/29.10.2020, HUS/58/2020). These temporal bones were dissected at the Department of Forensic Medicine, Helsinki University with the permission of National Supervisory Authority for Welfare and Health (permission no. 6834/06.01.03.01/2013).

Consent for publication

Not applicable.

Availability of data

All the 3D models of the study in STL format can be found from an open-source database (<https://doi.org/10.5281/zenodo.7281752>). If needed, the other data of this research

project can be published within the framework of permits and legislation.

Further disclosure

Part of the findings has been presented in the 6th Congress of European ORL-HNS, Milan, Italy, October 29–November 2, 2022.

References

1. Luers JC, Hüttenbrink KB, 2016, Surgical anatomy and pathology of the middle ear. *J Anat*, 228(2):338–353.
<https://doi.org/10.1111/joa.12389>
2. Rondini-Gilli E, Grayeli AB, Borges Crosara PF, *et al.*, 2003, Ossiculoplasty with total hydroxylapatite prostheses anatomical and functional outcomes. *Otol Neurotol*, 24(4):543–547.
<https://doi.org/10.1097/00129492-200307000-00003>
3. Colletti V, Carner M, Colletti L, 2009, TORP vs round window implant for hearing restoration of patients with extensive ossicular chain defect. *Acta Otolaryngol*, 129(4):449–452.
<https://doi.org/10.1080/00016480802642070>
4. Alaani A, Raut VV, 2010, Kurz titanium prosthesis ossiculoplasty—Follow-up statistical analysis of factors affecting one year hearing results. *Auris Nasus Larynx*, 37(2):150–154.
<https://doi.org/10.1016/j.anl.2009.05.004>
5. Yung M, Smith P, 2010, Titanium versus nontitanium ossicular prostheses—A randomized controlled study of the medium-term outcome. *Otol Neurotol*, 31(5):752–758.
<https://doi.org/10.1097/MAO.0b013e3181de4937>
6. Babighian G, Albu S, 2011, Stabilising total ossicular replacement prosthesis for ossiculoplasty with an absent malleus in canal wall down tympanomastoidectomy—A randomised controlled study. *Clin Otolaryngol*, 36(6):543–549.
<https://doi.org/10.1111/j.1749-4486.2011.02406.x>
7. Hess-Erga J, Møller P, Vassbotn FS, 2013, Long-term hearing result using Kurz titanium ossicular implants. *Eur Arch Otorhinolaryngol*, 270(6):1817–1821.
<https://doi.org/10.1007/s00405-012-2218-x>
8. Chen Z, Sun X, Zhou H, *et al.*, 2014, Comparison of hearing results of malleovestibulopexy and total ossicular replacement prosthesis for chronic otitis media patients with a mobile stapes footplate. *Ann Otol Rhinol Laryngol*, 123(5):343–346.
<https://doi.org/10.1177/0003489414526366>
9. Fayad JN, Ursick J, Brackmann DE, *et al.*, 2014, Total ossiculoplasty: Short- and long-term results using a

- titanium prosthesis with footplate shoe. *Otol Neurotol*, 35(1):108–113.
<https://doi.org/10.1097/MAO.0b013e3182a475ac>
10. Roux A, Bakhos D, Villeneuve A, *et al.*, 2015, Does checking the placement of ossicular prostheses via the posterior tympanotomy improve hearing results after cholesteatoma surgery? *Otol Neurotol*, 36(9):1499–1503.
<https://doi.org/10.1097/mao.0000000000000840>
 11. Atila NE, Kilic K, Sakat MS, *et al.*, 2016, Stabilization of total ossicular replacement prosthesis using cartilage “shoe” graft. *Am J Otolaryngol*, 37(2):74–77.
<https://doi.org/10.1016/j.amjoto.2015.12.001>
 12. Gostian AO, Kouamé JM, Bremke M, *et al.*, 2016, Long-term results of the cartilage shoe technique to anchor a titanium total ossicular replacement prosthesis on the stapes footplate after type III tympanoplasty. *JAMA Otolaryngol Head Neck Surg*, 142(11):1094–1099.
<https://doi.org/10.1001/jamaoto.2016.2118>
 13. O’Connell BP, Rizk HG, Hutchinson T, *et al.*, 2016, Long-term outcomes of titanium ossiculoplasty in chronic otitis media. *Otolaryngol Head Neck Surg*, 154(6):1084–1092.
<https://doi.org/10.1177/0194599816633669>
 14. Ulku CH, 2017, Endoscopy-assisted ear surgery for treatment of chronic otitis media with cholesteatoma, adhesion, or retraction pockets. *J Craniofac Surg*, 28(4):1017–1020.
<https://doi.org/10.1097/scs.00000000000003671>
 15. Wood CB, Yawn R, Lowery AS, *et al.*, 2019, Long-term hearing outcomes following total ossicular reconstruction with titanium prostheses. *Otolaryngol Head Neck Surg*, 161(1):123–129.
<https://doi.org/10.1177/0194599819831284>
 16. Gottlieb PK, Li X, Monfared A, *et al.*, 2016, First results of a novel adjustable-length ossicular reconstruction prosthesis in temporal bones. *Laryngoscope*, 126(11):2559–2564.
<https://doi.org/10.1002/lary.25901>
 17. Hirsch JD, Vincent RL, Eisenman DJ, 2017, Surgical reconstruction of the ossicular chain with custom 3D printed ossicular prosthesis. *3D Print Med*, 3(1):7.
<https://doi.org/10.1186/s41205-017-0015-2>
 18. Stoppe T, Bornitz M, Lasurashvili N, *et al.*, 2018, Function, applicability, and properties of a novel flexible total ossicular replacement prosthesis with a silicone coated ball and socket joint. *Otol Neurotol*, 39(6):739–747.
<https://doi.org/10.1097/mao.0000000000001797>
 19. Stoppe T, Bornitz M, Lasurashvili N, *et al.*, 2017, Middle ear reconstruction with a flexible prosthesis. *Curr Dir Biomed Eng*, 3:143–146.
<https://doi.org/10.1515/cdbme-2017-0030>
 20. Milazzo M, Danti S, Inglese F, *et al.*, 2017, Ossicular replacement prostheses from banked bone with ergonomic and functional geometry. *J Biomed Mater Res B Appl Biomater*, 105(8):2495–2506.
<https://doi.org/10.1002/jbm.b.33790>
 21. Hillman TA, Shelton C, 2003, Ossicular chain reconstruction: Titanium versus plastipore. *Laryngoscope*, 113(10):1731–1735.
<https://doi.org/10.1097/00005537-200310000-00013>
 22. Zhang LC, Zhang TY, Dai PD, *et al.*, 2011, Titanium versus non-titanium prostheses in ossiculoplasty: A meta-analysis. *Acta Otolaryngol*, 131(7):708–715.
<https://doi.org/10.3109/00016489.2011.556662>
 23. Dalchow CV, Grün D, Stupp HF, 2001, Reconstruction of the ossicular chain with titanium implants. *Otolaryngol Head Neck Surg*, 125(6):628–630.
<https://doi.org/10.1067/mhn.2001.120397>
 24. Truy E, Naiman AN, Pavillon C, *et al.*, 2007, Hydroxyapatite versus titanium ossiculoplasty. *Otol Neurotol*, 28(4):492–498.
<https://doi.org/10.1097/01.mao.0000265203.92743.d1>
 25. Coffey CS, Lee FS, Lambert PR, 2008, Titanium versus nontitanium prostheses in ossiculoplasty. *Laryngoscope*, 118(9):1650–1658.
<https://doi.org/10.1097/MLG.0b013e31817bd807>
 26. Redaelli de Zinis LO, 2008, Titanium vs hydroxyapatite ossiculoplasty in canal wall down mastoidectomy. *Arch Otolaryngol Head Neck Surg*, 134(12):1283–1287.
<https://doi.org/10.1001/archotol.134.12.1283>
 27. Ocak E, Beton S, Meço C, *et al.*, 2015, Titanium versus hydroxyapatite prostheses: Comparison of hearing and anatomical outcomes after ossicular chain reconstruction. *Turk Arch Otorhinolaryngol*, 53(1):15–18.
<https://doi.org/10.5152/tao.2015.775>
 28. Mäkitie AA, Salmi M, Lindford A, *et al.*, 2016, Three-dimensional printing for restoration of the donor face: A new digital technique tested and used in the first facial allotransplantation patient in Finland. *J Plast Reconstr Aesthet Surg*, 69(12):1648–1652.
<https://doi.org/10.1016/j.bjps.2016.09.021>
 29. Tuomi J, Paloheimo KS, Vehviläinen J, *et al.*, 2014, A novel classification and online platform for planning and documentation of medical applications of additive manufacturing. *Surg Innov*, 21(6):553–559.
<https://doi.org/10.1177/1553350614524838>
 30. VanKoevering KK, Hollister SJ, Green GE, 2017, Advances in 3-dimensional printing in otolaryngology: A review. *JAMA Otolaryngol Head Neck Surg*, 143(2):178–183.
<https://doi.org/10.1001/jamaoto.2016.3002>

31. Soetedjo AAP, Lee JM, Lau HH, *et al.*, 2021, Tissue engineering and 3D printing of bioartificial pancreas for regenerative medicine in diabetes. *Trends Endocrinol Metab*, 32(8):609–622.
<https://doi.org/10.1016/j.tem.2021.05.007>
32. Bandyopadhyay A, Mitra I, Bose S, 2020, 3D printing for bone regeneration. *Curr Osteoporos Rep*, 18(5):505–514.
<https://doi.org/10.1007/s11914-020-00606-2>
33. Brunello G, Sivoletta S, Meneghello R, *et al.*, 2016, Powder-based 3D printing for bone tissue engineering. *Biotechnol Adv*, 34(5):740–753.
<https://doi.org/10.1016/j.biotechadv.2016.03.009>
34. Kamrava B, Gerstenhaber JA, Amin M, *et al.*, 2017, Preliminary model for the design of a custom middle ear prosthesis. *Otol Neurotol*, 38(6):839–845.
<https://doi.org/10.1097/mao.0000000000001403>
35. Milazzo M, Muyschondt PGG, Carstensen J, *et al.*, 2020, De novo topology optimization of total ossicular replacement prostheses. *J Mech Behav Biomed Mater*, 103:103541.
<https://doi.org/10.1016/j.jmbbm.2019.103541>
36. Akmal JS, Salmi M, Hemming B, *et al.*, 2020, Cumulative inaccuracies in implementation of additive manufacturing through medical imaging, 3D thresholding, and 3D modeling: A case study for an end-use implant. *Appl Sci*, 10(8):2968.
<https://doi.org/10.3390/app10082968>
37. Chekurov S, Salmi M, Verboeket V, *et al.*, 2021, Assessing industrial barriers of additively manufactured digital spare part implementation in the machine-building industry: A cross-organizational focus group interview study. *J Manuf Technol Manag*, 32(4):909–931.
<https://doi.org/10.1108/JMTM-06-2020-0239>
38. Verboeket V, Khajavi SH, Krikke H, *et al.*, 2021, Additive manufacturing for localized medical parts production: A case study. *IEEE Access*, 9:25818–25834.
<https://doi.org/10.1109/ACCESS.2021.3056058>
39. Valtonen I, Rautio S, Salmi M, 2022, Capability development in hybrid organizations: Enhancing military logistics with additive manufacturing. *Progr Addit Manuf*, 7(5):1–16.
<https://doi.org/10.1007/s40964-022-00280-z>
40. Heiland KE, Goode RL, Asai M, *et al.*, 1999, A human temporal bone study of stapes footplate movement. *Am J Otol*, 20(1):81–86.
41. Hato N, Stenfelt S, Goode RL, 2003, Three-dimensional stapes footplate motion in human temporal bones. *Audiol Neurootol*, 8(3):140–152.
<https://doi.org/10.1159/000069475>
42. Sim JH, Chatzimichalis M, Lauxmann M, *et al.*, 2010, Complex stapes motions in human ears. *J Assoc Res Otolaryngol*, 11(3):329–341.
<https://doi.org/10.1007/s10162-010-0207-6>
43. Kemp P, Stralen JV, De Graaf P, *et al.*, 2020, Cone-beam CT compared to multi-slice CT for the diagnostic analysis of conductive hearing loss: A feasibility study. *J Int Adv Otol*, 16(2):222–226.
<https://doi.org/10.5152/iao.2020.5883>